HHS Public Access

Author manuscript

Exp Cell Res. Author manuscript; available in PMC 2023 May 01.

Published in final edited form as:

Exp Cell Res. 2022 May 01; 414(1): 113083. doi:10.1016/j.yexcr.2022.113083.

Evidence that the transcriptional repressor ICER is regulated via the N-end rule for ubiquitination

Angelo Cirinelli[1,3,*], **Justin Wheelan**[1,2,*], **Christopher Grieg**[1,3], **Carlos A. Molina**[1,2]

[1]Department of Biology, Montclair State University, Montclair, NJ 07043

[2]Environmental Science and Management Program, Montclair State University, Montclair, NJ 07043

[3]Molecular Biology and Genetics Program, Rutgers New Jersey Medical School, Newark, NJ 07103

Abstract

ICER is a transcriptional repressor that is mono- or poly-ubiquitinated. This either causes ICER to be translocated from the nucleus, or degraded via the proteasome, respectively. In order to further studies the proteins involved in ICER regulation mass spectrometry analysis was performed to identify potential candidates. We identified twenty eight ICER-interacting proteins in human melanoma cells, Sk-Mel-24. In this study we focus on two proteins with potential roles in ICER proteasomal degradation in response to the N-end rule for ubiquitination: the N-alpha-acetyltransferase 15 (NAA15) and the E3 ubiquitin-protein ligase UBR4. Using an HA-tag on the N- or C-terminus of ICER ($_{N}$HAICER or ICER$_{C}$HA) it was found that the N-terminus of ICER is important for its interaction to UBR4, whereas NARG1 interaction is independent of HA-tag position. Silencing RNA experiments show that both NAA15 and UBR4 up-regulates ICER levels and that ICER's N-terminus is important for this regulation. The N-terminus of ICER was found to have dire consequences on its regulation by ubiquitination and cellular functions. The half-life of $_{N}$HA-ICER was found to be about twice as long as ICER$_{C}$HA. Polyubiquitination of ICER was found to be dependent on its N-terminus and mediated by UBR4. This data strongly suggests that ICER is ubiquitinated as a response to the N-end rule that governs protein degradation rate through recognition of the N-terminal residue of proteins. Furthermore, we found that $_{N}$HA-ICER inhibits transcription two times more efficiently than ICER$_{C}$HA, and causes apoptosis 5 times more efficiently than ICER$_{C}$HA. As forced expression of ICER has been shown before to block

Address correspondence: Carlos A. Molina, Ph.D., Department of Biology, Montclair State University, 1 Normal Avenue, Montclair, NJ 07043, Tel: (973) 655-3302, Fax: (973) 655-7047, molinac@montclair.edu.

*Contributed equally to this manuscript

Carlos A. Molina: Conceptualization, Investigation, Writing - Original Draft, Supervision, Project administration, Funding acquisition

Angelo Cirinelli: Conceptualization, Investigation, Writing - Original Draft, Writing - Review & Editing

Justin Wheelan: Conceptualization, Investigation, Writing - Original Draft, Writing - Review & Editing

Christopher Grieg: Conceptualization, Investigation

Declarations of interest: none

cells in mitosis, our data represent a potentially novel mechanism for apoptosis of cells in mitotic arrest.

Keywords

ICER; Cancer; Ubiquitination; N-end rule; NAA15; UBR4

Introduction

According to the Center for Disease Control and Prevention skin cancer is the most prominent cancer in the United States (1). Melanoma is a malignancy that develops from the pigment producing cells, melanocytes (2). Despite being a rare type of skin cancer, it is responsible for the vast majority of skin cancer-related deaths (3). Moreover, metastatic melanoma is one of the most highly mutated, heterogeneous and lethal types of cancer (4). In recent years treatments for advanced-stage melanoma have improved greatly with the development of BRAF and MEK inhibitors, blocking antibodies to cytotoxic T-lymphocyte-associated antigen 4, programmed cell-death protein 1 (PD-1) and PD-1 ligand, and a modified oncolytic herpes virus that is delivered intratumorally (5,6). These landmark changes in practice came with the unforeseen reality that the majority of patients are either intrinsically resistant or rapidly acquire resistance to treatment (6,7). The lack of response can be driven by mutations and non-mutational events in tumor cells, as well as by changes in the surrounding tumor microenvironment.(6, 7, 8–14).

Amongst the many non-mutational events associated with resistance to treatments of melanoma, the importance of the cAMP pathway and the transcription factors involved in this pathway has been highlighted in the development of resistance to BRAF/MEK inhibitors (8,9). For instance, a study performed with a BRAF(V600E) melanoma cell line treated with RAF, MEK, ERK or combined RAF-MEK inhibitors revealed that a cyclic-AMP dependent signaling pathway in melanoma was associated with drug resistance (8). In addition, cAMP response element binding protein (CREB), was involved; with CREB being found to be suppressed by RAF-MEK inhibition in BRAF(V600E) melanoma biopsies, but restored in relapsing tumors. It is hypothesized that ICER, as a repressor of gene expression (an antagonist of CREB) of the cAMP pathway, might be involved in this observed resistance to BRAF/MEK inhibitors in relapsing melanomas.

ICER (Inducible cAMP Early Repressor), a family of four different isoforms, referred to collectively as ICER for convenience, is an inducible transcription factor that originates from within the *CREM (cAMP Response Element Modulator)* gene and is a strong repressor of cAMP-mediated gene expression (15,16). ICER contains a short and conserved N-terminal sequence, encoded by exon X, followed by a γ-domain (absent in γ-isoforms ICER γI and ICER γII) and one of the DNA binding domains encoded by exon H and exon Ia (ICER I) or Ib (ICER-II) in the *Crem* gene.

Forced expression of ICER arrests cells at the G1/S and G2/M boundaries of the cell cycle, by downregulating expression of relevant proteins involved in the cellular proliferation such as cyclin A, c-fos and cyclin D1 and sufficient to inhibit cell growth in an anchorage-

independent manner and prevent tumorigenesis in nude mice (17–19). In addition to its apparent involvement in cell cycle regulation, it has been demonstrated that ICER is down-regulated in melanomagenesis, but is strongly up-regulated in melanoma regression (18). ICER mRNA expression is unaffected in cancer cells, suggesting that the observed down regulation of ICER is *not* the result of a genetic alteration, but rather post-translational modifications (i.e., phosphorylation and ubiquitination) (20, 21). Previously, we have demonstrated that ICER proteasomal degradation is implicated in Ras/MAPK-mediated melanoma tumorigenesis using Tyr/Tet-Ras INK4a−/− transgenic mice and melanoma cells (R545 cells) in culture isolated from Tyr/Tet-Ras INK4a−/− mice. In these models, melanoma genesis and melanoma maintenance is strictly dependent upon expression of H-RasV12G and in fact, pharmacological inhibition of Ras activity or the proteasome abolished the degradation of ICER caused by H-RasV12G expression indicating that RAS oncogene regulates the expression of ICER protein by targeting ICER for proteasomal degradation (18). Taken together, ICER plays a critical role regulating oncogenesis, though no studies to date have identified the exact mechanisms and ubiquitin ligases involved in ICER post-translational regulation.

In this report, using liquid chromatography-tandem mass spectrometry (LC-MS/MS), we identified two candidate proteins NAA15 and UBR4 which have been shown to play an important role in what is known as the N-end rule pathway (22–27). The N-end rule pathway is a proteolytic system in which N-terminal residues of short-lived proteins are recognized by recognition components (N-recognins) as essential components of degrons, called N-degrons. N-recognins-mediate protein ubiquitination and selective proteolysis by the 26S proteasome (22). The N-end rule pathway mediates recognition of the N-terminus of substrate proteins by a family of N-terminal-acetylases that catalyze the attachment of an acetyl moiety from acetyl-CoA to the N-termini of the cellular proteins (23). Of note, the gene for NAA15 encodes the auxiliary subunit of the N-terminal acetyltransferase A (NatA) complex (26, 27). The human NatA complex co-translationally acetylates N-termini that bear a small amino acid, which is exposed after methionine cleavage by methionine aminopeptidases (28–31).

Our data suggests that ICER N-terminus is important for recognition by enzymes responsible for the N-end rule of ubiquitination and proteasomal degradation with consequences for the regulation of apoptosis. Altogether, this information has ramifications for ICER to target the cAMP pathway in drug resistance tumors by eliciting apoptosis.

Materials and Methods

Cells, plasmids, Western blot (WB), immunoprecipitation (IP), Co-immunoprecipitation (CoIP), antibodies, chemicals and siRNAs

SK-MEL-24 (ATCC® HTB-71™) human melanoma cells were purchased from ATCC and cultured as recommended. pcDNA3.1™(+) or pSV40 plasmids were used for ICER-Iγ expression with HA-tag or on N- or C-terminus. pEGFPN1 and pEGFPC1 were used for enhanced green fluorescent protein (EGFP) expression and for the expression with EGFP-tag on N- or C-terminus of ICER-Iγ. pMTCEV was used as an expression vector for the catalytic subunit of PKA (21). ICER expression under the SV40 promoter (pSV40) was

constructed using pRL-SV40 plasmid (purchased from Promega). The Renilla luciferase gene was replaced with $_{N}$HA-ICER or ICER$_{C}$HA into unique NheI and XbaI sites on pRL-SV40 plasmid.

Sodium dodecyl sulfate polyacrylamide gel electrophoresis (SDS-PAGE) and WB analysis were performed as described before (19, 20, 21) or as recommended by the various suppliers of antibodies. WB detection and quantification was performed using IRDye® secondary antibodies and imaged using the Odyssey® CLx infrared system from LI-COR. Rabbit Anti-HA and anti-ubiquitin monoclonal antibodies (Ubi-1) were purchased from Invitrogen (Catalog No. 71–5500 and 13–1600) and used as directed for WB and Immunocytochemistry (ICC). Co-immunoprecipitation was performed using Pierce® HA Tag IP/Co-IP kit as directed by the manufacturer. GFP-Trap magnetic agarose was purchased from ChromoTek Inc. and used as directed for the precipitation of EGFP-tagged proteins. Tubulin antibodies (TU-02) was purchased from Santa Cruz Biotechnology and used as directed for WB. Anti-NARG1 (ab60065), Anti-UBR4/P600 (ab86738) and anti-GFP (ab6556) antibodies were purchased from ABCAM and used as directed. The MG132 (M7449) and cycloheximide (C4859) were purchased from Sigma-Aldrich. FuGENE®HD Transfection Reagent was purchased from Promega and used as directed for cell transfection following the 8:2 ratio of Fugene:DNA protocol. All siRNAs were ordered from Ambion by Life Technologies as Silencer® Pre-designed (Inventoried) as annealed siRNA. The sense and antisense sequences (5'–3') of the oligonucleotides as designed by the manufacturer are; for NAA15: GGUCAGACAAGAAGUAUGAtt and UCAUACUUCUUGUCUGACCtc, for UBR4: GCAGUACGAGCCAUUCUACtt and GUAGAAUGGCUCGUACUGCtt. siRNA transfections were performed using the reagents and protocol from Lipofectamine® RNAiMAX reagents from Life Technologies. Samples were collected 24 hours after siRNA transfection. As a negative control cells were transfected with a validated Silencer™ Negative Control No. 1 siRNA (AM4611). For the experiments where the expression of transfected ICER$_{C}$HA and $_{N}$HA-ICER was analyzed by WB after siRNA, cells were first transfected using the DNA constructs with the pSV40 plasmids mentioned above. After 48 hours transfected cells were split into 8 wells of 6-well dishes. 24 hours later, cells were transfected with the siRNAs and samples collected 24 hours after siRNA transfection.

In-gel digestion, liquid chromatography-tandem mass spectrometry (LC-MS/MS) and database Search

After Co-IP and SDS-PAGE the coomassie gel plugs were sent to the Mass Spectrometry (MS) Facility, Center for Advanced Biotechnology and Medicine, Rutgers University, Piscataway, NJ, USA for in-gel digestion, LC-MS/MS and data analysis following previously described protocols (32, 33). Each gel band was subjected to reduction with 10mM DTT for 30 min at 60°C, alkylation with 20mM iodoacetamide for 45min at room temperature in the dark and digestion with 0.2μg trypsin (sequencing grade, ThermoScientific Cat#90058), and incubated overnight at 37°C. Peptides were extracted twice with 5% formic acid, 60% acetonitrile and dried under vacuum. Samples were analyzed by LC-MS using Nano LC-MS/MS (Dionex Ultimate 3000 RLSCnano System, Thermofisher) interfaced with Eclipse (ThermoFisher). 3 μL out of 12.5μLl of in-gel digested Sample P was loaded onto a fused silica trap column (Acclaim PepMap 100,

75μmx2cm, ThermoFisher). After washing for 5 min at 5 μl/min with 0.1% TFA, the trap column was brought in-line with an analytical column (Nanoease MZ peptide BEH C18, 130A, 1.7um, 75μmx250mm, Waters) for LC-MS/MS. Peptides were fractionated at 300 nL/min using a segmented linear gradient 4–15% B in 30min (where A: 0.2% formic acid, and B: 0.16% formic acid, 80% acetonitrile), 15–25%B in 40min, 25–50%B in 44min, and 50–90%B in 11min. Solution B then returns at 4% for 5 minutes for the next run. The scan sequence began with an MS1 spectrum (Orbitrap analysis, resolution 120,000, scan range from M/Z 375–1500, automatic gain control (AGC) target 1E6, maximum injection time 100 ms). The top S (3 sec) duty cycle scheme was used to determine the number of MSMS performed for each cycle. Parent ions of charge 2–7 were selected for MSMS and dynamic exclusion of 60 seconds was used to avoid repeat sampling. Parent masses were isolated in the quadrupole with an isolation window of 1.2 m/z, automatic gain control (AGC) target 1E5, and fragmented with higher-energy collisional dissociation with a normalized collision energy of 30%. The fragments were scanned in Orbitrap with resolution of 15,000. The MSMS scan ranges were determined by the charge state of the parent ion but lower limit was set at 110 amu.

The peak list of the LC-MSMS were generated by Thermo Proteome Discoverer (v. 2.1) into MASCOT Generic Format (MGF) and searched against the uniprot human database as well as a database composed of common lab contaminants using an in house version of X!Tandem (GPM Fury1). Search parameters are as follows: fragment mass error, 20 ppm; parent mass error, +/− 7 ppm; fixed modification, carbamidomethylation on cysteine; variable modifications: methionine mono-oxidation for the primary search, asparagine deamination, tryptophan oxidation and di-oxidation, Methionine di-oxidation, and glutamine to pyro-glutamine were considered at the refinement stage. Protease specificity: trypsin (C-terminal of R/K unless followed by P with 1 missed cleavage during the preliminary search and 5 missed cleavages during refinement. Minimum acceptable peptide and protein expectation scores were set at 10^{-2} and 10^{-4}, respectively.

Half-life determination, nuclear and cytoplasmic cell fractionation and immunocytochemistry (ICC)

Half-life experiments were performed as described before (20) with the following modifications. Forty eight hours after transfection, cells were treated with10 μg/mL cycloheximide (CHX) to block de-novo protein synthesis. Cells were then collected at 0, 1, 3 and 6 hours after block and samples analysed by WB and quantified as described above. Cell fractionations were performed using NE-PER nuclear and cytoplasmic extraction reagents kit purchased from Pierce/Thermo Scientific (78833) following their protocol. ICC was performed using 4μg/mL of the Rabbit Anti-HA antibody as mentioned above using a 1:2000 dilution of Donkey anti-rabbit IgH (A-21206) from ThermoFisher following the manufacturer's protocol.

Site-directed mutagenesis (SDM).

SDM was performed using the QuikChange II Site-Directed Mutagenesis Kit (200523) from Agilent Technologies. The primers shown below in parentheses were used for the deletion of the first N-terminus eight amino acids of ICER protein (MAVTGDET) and substituted

by a new initiator methionine. pcDNA3.1™(+) plasmid containing ICER$_C$HA cDNA was used as the template for SDM. After the SDM reaction the mutation was confirmed by DNA sequencing. (Primers for SDM: accgagctcggatccattgccgtgacaggcgacgagacaatgagcgccaccacag and inverse complimentary primer).

Electrophoretic Mobility Shift Assay (EMSA), Chromatin immunoprecipitation (ChIP), Luciferase assay and DeadEnd Fluorometric TUNEL assay

EMSA was performed as described before (15,16) however in this experiment, we used the Odyssey® Infrared EMSA kit from LI-COR (829–07910) and a CREB IRDye® 700 Infrared labeled oligonucleotides containing a canonical CRE (5'TGACGTCA3') (829–07923) following the manufacturer protocol. For supershift determinations, samples were co-incubated with Rabbit anti-HA (Invitrogen) for 10 minutes before running the samples on native gels.

SimpleChIP® Enzymatic Chromatin IP Kit (9003) was used for ChIP assays following the manufacturer protocol and previously described protocol (34, 35) IgG was supplied with the ChIP assay kit. Anti-HA tag antibody-ChIP grade (ab9110) were purchased from ABCAM. The oligonucleotides used to amplify a 151bp sequence of the human cyclinD2 promoter containing a CRE at position −294 were (5'−3'): GAAAGGGGAGGAGGAACCAGAG and CTGCCTCACTCGCACCG.

Luciferase assay was performed as described before (21) using DUAL Luciferase® reporter assay system from Promega (E1910) was used following their specifications and performed using the firefly luciferase reporter gene with the wild type human cyclin D1 promoter as previously described (34).

DeadEnd™ Fluorometric TUNEL (TdT-mediated dUTP Nick-End Labeling) assay from Promega (TB235) was performed following the manufacturer protocol and specifications.

Results/Discussion

Identification of ICER-interacting proteins.

In order to identify ICER-interacting proteins, mass spectrometry (MS) was performed after co-immunoprecipitation (Co-IP) of ICER-expressing cell extracts. SK-MEL-24 cells were transfected with a plasmid encoding ICER with an HA-tag on its C-terminus (ICER$_C$HA). As a control, cells were transfected with a plasmid encoding EGFP. Cells were treated with +/− proteasome inhibitor MG-132 in order to obtain accumulation of ICER as shown before (18, 20). The expression of ICER$_C$HA was confirmed by WB of cell extracts containing 3μg of the total protein (See Figure 1A). Using the same samples, ICER$_C$HA was immunoprecipitated from extracts containing 600μg of total protein. Samples were analyzed by SDS-PAGE and Coomassie blue staining to confirm the quantity and quality of the samples (Figure 1B). The identity of the immunoprecipitated bands was further analyzed by WB of an aliquot of the immunoprecipitated samples (Figure 1C). This was necessary to demonstrate that ICER$_C$HA was efficiently and specifically immunoprecipitated from transfected SK-MEL-24 cells in order to perform MS analysis.

For further purification for MS analysis, the Co-IP samples (prepared as described above and in “Material and Methods”) were loaded onto a SDS-PAGE, separated by 0.5–1cm into the gel and stained with Coomassie blue (Figure 1D). The stained gels plugs were excised and sent for MS analysis to the Mass Spectrometry Facility, Center for Advanced Biotechnology and Medicine, Rutgers University. Three samples were analyzed after IP with agarose-linked anti-Ha antibodies: ICER$_C$HA with or without MG132 treatment and EGFP control.

Putative Co-IP proteins were evaluated by spectral count as semi-quantitative values to determine ICER-specific interactions. Twenty eight proteins were detected in the Co-IP sample that interact specifically with ICER$_C$HA (Table 1). Several identified peptides are bona-fide ICER interacting proteins, such as CREM, Transportin-1, Importin subunit beta-1, Importin-7, and Proteasome subunit beta type-1, −3 and −5 and ICER itself (not shown). We focused on two identified proteins with potential roles on ICER ubiquitination: N-alpha-acetyltransferase 15 (NAA15) and E3 ubiquitin-protein ligase UBR4 because we hypothesized that these peptides are involved in ICER ubiquitination and regulation through the N-end rule of ubiquitination (22–27).

NAA15 and UBR4 interact with and regulate ICER protein levels

Co-immunoprecipitation and WB were performed to validate the interaction between ICER and NAA15 and UBR4. SK-Mel-24 cells were transfected with plasmids expressing EGFP, ICER$_C$HA or ICER with the HA tag on its N-terminus ($_N$HA-ICER). The expression of ICER was confirmed by WB using anti-HA antibodies before and after immunoprecipitation. As shown in Figure 2, both ICER$_C$HA and $_N$HA-ICER have similar expression profiles and inhibition of the proteasome resulted in an accumulation of both ICER$_C$HA and $_N$HA-ICER. NAA15 was co-immunoprecipitated with both ICER$_C$HA and $_N$HA-ICER (Figure 2C). By contrast, UBR4 was principally present in samples precipitated from cells transfected with ICER$_C$HA, suggesting that the N-terminus of ICER is important for interaction with UBR4, whereas NAA15 interaction is independent of the position of the HA-tag.

Endogenous ICER protein levels were measured via WB after inhibiting the expression of NAA15 and UBR4 by siRNA (Figure 3). Inhibition of NAA15 resulted in a 1.3-fold induction on ICER expression, whereas UBR4 inhibition resulted in 2.2-fold induction relative to the control (Figure 3B). In order to examine the importance of the N-terminus of ICER on ICER levels, cells were first transfected with a plasmid expressing either ICER$_C$HA or $_N$HA-ICER and then treated with siRNA oligos to block the expression of NAA15 and UBR4 as before. Figure 3C shows that only ICER$_C$HA levels were affected by siRNA knockdown in a similar manner as for endogenous ICER in Figure 3B. It is important to note that knockdown of UBR4 rescued ICER levels with the highest intensity. This data further supports the role of these enzymes on controlling ICER protein expression and strongly suggests that the N-terminus of ICER is critical for post-translational regulation.

The N-terminus dictates ICER stability and UBR4 ubiquitin-mediated proteasomal degradation.

In order to determine if the N-terminus of ICER affects its stability, the half-life of $ICER_CHA$ and $_NHA$-ICER was compared. Figure 4 shows that $_NHA$-ICER half-life is almost 2 hours longer than the half-life of $ICER_CHA$. In conjunction with the data presented in figures 2 and 3, we posit that the N-terminus of ICER is recognized by UBR4 affecting ICER ubiquitination and proteasomal degradation. Indeed the data presented in Figures 5 confirmed this supposition. Figure 5A demonstrates that $ICER_CHA$ is polyubiquitinated, whereas $_NHAICER$ is not. Similarly, the levels of polyubiquitinated ICER with an EGFP tag on its C-terminus ($ICER_CEGFP$) accumulates upon inhibition of the proteasome, but $_NEGFP$-ICER (ICER with EFGP on its N-terminus) does not gets polyubiquitinated (Figure 5B).

In order to investigate whether UBR4 mediates the ubiquitination of ICER, cells were transfected with $ICER_CHA$ and $_NHA$-ICER, with or without silencing UBR4 protein levels and in the presence or absence of a proteasome inhibitor. Figure 5C shows that if UBR4 levels are diminished by gene silencing, the levels of polyubiquitinated $ICER_CHA$ are also abrogated. This diminishing in polyubiquitination was only observed with $ICER_CHA$ but not $_NHA$-ICER. These results demonstrate that UBR4 is a E3 ubiquitin ligase for ICER that recognizes ICER N-terminus for polyubiquitination and subsequent proteasomal degradation. Of interest is the fact that the silencing of UBR4 leads to an increase in the polyubiquitination of ICER when cells are not treated with MG132. This may suggest that there are other ubiquitin ligases involved in the regulation of ICER, which may be uncovered in future studies.

In order to further study the role of the N-terminus of ICER in dictating its ubiquitination, an N-terminus mutated ICER was constructed. This mutated ICER termed here ΔN_8-$ICER_CHA$ lacks the first 8 amino acids representing the amino acids encoded by the ICER-specific exon X (5,6). Figure 6 shows that polyubiquitinated intermediates of ΔN_8-$ICER_CHA$ do not accumulate as for $ICER_CHA$ when the proteasome is inhibited. Furthermore, Figure 6A shows that ΔN-$ICER_CHA$ migrates at a similar molecular weight as a smaller HA-tagged peptide that always accompanies $ICER_CHA$ and not $_NHA$-ICER (see band labeled with a ? symbol in Figures 1, 2, 4 and 5). Mass spec analysis of this peptide after immunoprecipitation demonstrates that this peptide corresponds to $ICER_CHA$ lacking the first four N-terminus amino acids (MAVT) of ICER. In this report this modified form of ICER is termed ΔN_4-$ICER_CHA$. The existence of ΔN_4-$ICER_CHA$ is in congruence with modifications of proteins at the N-terminus in response to the N-end rule of ubiquitination (22–31).

ICER tags do not affect nuclear functions as a transcriptional repressor.

ICER is a transcription factor with a strong nuclear localization signal (NLS) (15, 16). The effect of the HA-tag on ICER subcellular localization was studied by ICC and direct fluorescence microscopy of transfected cells with plasmids expressing $_NHA$-ICER, $ICER_CHA$, $_NEGFP$-ICER or $ICER_CEGFP$. The ICC in Figure 7A shows that the location of the HA-tag does not affect ICER nuclear localization. In fact, both $ICER_CHA$ and $_NHA$-

ICER are almost exclusively nuclear. The observed nuclear localization of $_{N}$EGFP-ICER and ICER$_{C}$EGFP in Figure 7B confirmed these observations. Since ICER's NLS is within ICER's primary sequence, it is not surprising that the HA-tag or EGFP-tag on the N- or C-terminus does not interfere with ICER mostly nuclear localization.

Given that ICER is part of the family of transcription factors that binds DNA using a basic leucine-zipper motif (15, 16), we wanted to compare the ability of ICER$_{C}$HA and $_{N}$HA-ICER to bind a canonical CRE by electrophoretic mobility shift assay (EMSA) (Figure 8). It was observed that both ICER$_{C}$HA and $_{N}$HA-ICER bind to DNA with similar affinities in an in vitro DNA binding assay. In order to assess ICER DNA binding affinity in cells, a ChIP assay was performed. Figure 8B demonstrates that in cells, both ICER$_{C}$HA and $_{N}$HA-ICER seem to bind the CRE in *CCND2* (cyclin D2) promoter indistinguishably. Figures 8A and B demonstrated that the location of the HA-tag does not interfere with ICER DNA binding capability.

It was then postulated that the location of the HA-tag on ICER may affect its activity as a transcriptional repressor. To test this hypothesis a luciferase assay was performed using the *CCND2* promoter as the read out for transcriptional activity. Figure 8C shows that both ICER$_{C}$HA and $_{N}$HA-ICER repress the expression of *CCND2* promoter with different efficiencies. When cells were transfected with 50ng of each plasmid, the repression observed with $_{N}$HA-ICER was twice as efficient as for ICER$_{C}$HA. In fact, $_{N}$HA-ICER repression was almost 100%, whereas ICER$_{C}$HA repression was only about 50% (Figure 8C). It is hypothesized that these differences in transcriptional repression may be due to the dissimilarity in half-life observed in figure 4. In support of this proposition, it was observed that doubling the amount of ICER$_{C}$HA (100ng of transfected plasmid DNA) caused repression levels to reach the same repression levels as for the transfected cells with 50ng of $_{N}$HA-ICER DNA. Similar results were observed when UBR4 expression was silenced by siRNA using 50ng of plasmid DNA. The data presented up to now support the notion that $_{N}$HA-ICER is a stronger transcriptional repressor not because of the ability to bind DNA but because it has a longer half life due to the inability of UBR4 to efficiently ubiquitinated $_{N}$HA-ICER and targeted to proteasomal degradation.

$_{N}$HA-ICER elicit a stronger apoptotic response than ICER$_{C}$HA

ICER has been shown to induce apoptosis in cell and animal models (36, 37). The potentiality of ICER$_{C}$HA and $_{N}$HA-ICER in causing apoptosis was determined in transiently transfected SK-MEL-24 human melanoma cells by Terminal deoxynucleotidyl transferase dUTP nick end labeling (TUNEL) assay. Figure 9 shows that $_{N}$HA-ICER is 5-times more potent than ICER$_{C}$HA in eliciting apoptosis measured by TUNEL assay. Since in Figure 4 it was observed that $_{N}$HA-ICER has a much longer half-life than ICER$_{C}$HA it is reasonable to postulate that these differences in apoptosis may be related to this phenomena. Indeed we observed that when the levels of UBR4 were silenced by siRNA, TUNEL-positive cells increased from 8 to 21% in ICER$_{C}$HA transfected cells, whereas UBR4 silencing does not increase TUNEL levels in $_{N}$HA-ICER or Luc control transfected cells.

Conclusions

The data presented in this report strongly support the hypothesis that ICER is ubiquitinated by UBR4 in response to the Ac/N-end rule pathway of ubiquitin mediated proteasomal degradation. In the Ac/N-end rule pathway, methionine aminopeptidases remove the N-terminal initiator methionine, if the residues smaller than Valine occupy the penultimate position. N-terminal acetylation targets proteins largely based on their first few residues. The Ac/N-recognins (like UBR4) specifically recognize the N-terminal acetyl moiety of the N-terminally acetylated proteins for polyubiquitin-mediated and proteasome-dependent degradation (22–31). ICER N-terminus sequence conforms with the predicted N-terminus amino acid sequence signal for the Ac/N-end rule pathway. As noted before, the first 8 amino acids (MAVTGDE/DT-) on ICER N-terminus are coded exon X (15, 16). This sequence is conserved between species (human, rodents, birds and fish) suggesting a generalized function for this canonical N-terminus among eukaryotes.

Even though we did not show direct data that NAA15 acetylate ICER in response to the N-end rule, data presented using gene silencing experiments strongly suggest that former scenario. In addition, the finding that the mass spec analysis described as part of Figure 6, identified an ICER-related peptide, ΔN-ICER$_c$HA lacking the first four N-terminus amino acids of ICER$_c$HA further support the postulate that amino acids ath the N-terminus of ICER are removed in response to N-terminal acetylation (22, 31).

A new isoform of ICER, termed small ICER (smICER) was identified lacking exon x (38) and hence ICER canonical N-terminus. SmICER is regulated by a newly identified promoter in the CREM gene. A genomic analysis for DNA binding sites between ICER and smICER demonstrated that the binding sites nearly completely overlap with a few ICER-specific and smICER-specific sites (39). Notably, the kinetics of transcriptional repression between ICER and smICER were shown to be different, with smICER having a longer repression times than ICER. It is reasonable to speculate that this observed difference might be related to different regulation by the enzymes responding to the N-end rule of proteasomal degradation. Although smICER appears to be an interesting new family member of transcription factors regulating the transcriptional control of the cAMP pathway, the physiological expression and functions of smICER protein is yet to be fully characterized.

ICER has been previously shown to be regulated by ubiquitination by other ub ligases in pituitary, testis and heart cells (20, 40, 41). None of these proteins were amongst those 28 found to Co-IP with ICER in the mass spec analysis of this report. One possibility is that there may be tissue-specific ubiquitination of ICER as in this report melanoma cells were used for the experiments. Another possibility is that different ICER isoforms are differentially regulated by ub ligases. If that is the case, the specific recognition of these other Ub ligases are in the DNA binding domain of ICER as all ICER isoforms coming from the P2 promoter of the CREM gene have the same N-termini (15, 16). The hypothesis put forward in this report indicating that ICER N-terminus is important for its regulation could be further investigated looking at the recently identified smICER that has an alternative N-terminus (38, 39).

ICER has been shown to elicit apoptosis (36, 37). In figure 9 of this report data is presented showing that $_{N}$HA-ICER caused apoptosis 5 times more efficiently than ICER$_{C}$HA. Further data presented in this report support the hypothesis that this is due to protection of ICER N-terminus from recognition by UBR4 ubiquitin ligases when tags were used. It has been shown that overexpression of ICER arrest cells in mitosis (42). In mitosis, ICER is monoubiquitinated after phosphorylation by the mitotic kinase CDK1 (21). A possible scenario that may explain this is as follows, overexpression of ICER causes apoptosis because such high levels of ICER proteins cannot be efficiently ubiquitinated causing apoptosis. It has been observed that prolonged mitotic arrested cells either die by apoptosis, or exit mitosis without dividing by a process known as slippage (43, 44). The pro-survival Bcl-2 family of proteins are emerging as a key player dictating the balance between these two fates (44). The *BCL2* promoter contains a functional CRE upstream of the translation start site (36). ICER has been shown to inhibit the expression of Bcl-2 by binding to this CRE (37) hence it is reasonable to postulate ICER as a positive mediator of apoptosis. A question yet to be answered is how many other gene promoters does ICER regulate that may also be related to apoptosis and why is ICER monoubiquitinated in mitosis. The specific mechanism on how ICER causes apoptosis are not yet fully understood. Further experimentation using genome wide approaches will clarify what set of apoptosis-related genes are regulated by ICER.

This report shows that ICER N-terminus is important for ICER protein regulation. The observation that when ICER N-terminus is protected by the HA-tag causes the half-life of ICER to double, suggesting the possibility of using this knowledge for the design of specific inhibitors to the UBR4 ubiquitin ligase. Interestingly a search for human proteins containing ICER N-terminus sequence (MAVTGD) using several common databases (Uniprot, Interpro, HHpred) resulted in no hits with the exception of ICER itself. These data and observations put forward the possibility to design small peptides based on N-terminus sequence of ICER to specifically inhibit UBR4 so endogenous ICER could then repress cell growth and elicit cell death.

ICER has previously shown to be both polyUb (20) and monoUb (21). Phosphorylation on a discrete serine residue (Ser 41) by ERK1 was a prerequisite for PolyUb, whereas phosphorylation on a different serine (Ser 35) by the mitotic kinase cdk1 was necessary for monoUb. It is tempting to speculate whether ICER might be mutually exclusive mono- or polyUb on its N-terminus. MonoUb of ICER in mitosis may protect ICER from polyUb-mediated proteasomal degradation, and affect binding to DNA. As the cells are entering G1, monoUb ICER might be deubiquitinated and re-localized to the nucleus reestablishing ICER DNA binding and its repressor activity. This hypothesis is further supported by the observation that the expression of ICER, monoUb ICER and polyUb ICER fluctuates during the cell cycle. Unmodified ICER was mostly observed in early G1, polyub in late G1/S and mono was only detected in mitotic cells (21). Future studies will conduct a more comprehensive analysis on the enzymes responsible for ICER post-translational modifications and the characterization of the ubiquitinated residues on ICER protein to further understand its role during the cell cycle and apoptosis.

The proteolytic Arg/N-degron pathway has been shown to be relevant to perturbations in cancer (45–47). Many components of this pathway are emerging as targets for anti-tumor therapies, because of its capacity to positively regulate many hallmarks of cancer, including angiogenesis, cell proliferation, motility, and survival. Selective downregulation of the four Arg/N-degron-dependent ubiquitin ligases, UBR1, UBR2, UBR4, and UBR5, demonstrated decreased cell migration and proliferation and increased spontaneous apoptosis in cancer cells (48). Whereas, NATs have been suggested to act as oncoproteins as well as tumor suppressors in human cancers, and NAT expression may be both elevated and decreased in cancer versus non-cancer tissues (49). Interesting NAA15 was originally discovered as a marker for gastric cancer and originally named as gastric cancer antigen Ga19 (50). At this time the regulation of these enzymes in melanoma and association with patient outcome is less well studied. The data represented shows a correlation for these enzymes in the regulation of ICER expression in melanoma cells. This study will be foundational to the development of novel targeted strategies to interfere with the ubiquitination-mediated degradation of antitumor proteins in order to restore normal expression levels in malignant cells eventually leading to their demise.

Acknowledgements

We would like to thank Haiyan Zheng, PhD for her assistance with the MS experiments. Colette Killian for ensuring that the Molina lab can work efficiently, and finally the students in the molecular biology II and advanced molecular biology classes for their assistance on these experiments.

Funding:

This work was supported by the National Institutes of Health [grant number 5SC1GM125583]

References:

1. Centers for Disease Control and Prevention. (Accessed 2021, August 2). Melanoma of the Skin Statistics. Centers for Disease Control and Prevention. https://www.cdc.gov/cancer/skin/statistics/index.htm
2. Shain AH, & Bastian BC (2016). From melanocytes to melanomas. Nature reviews. Cancer, 16(6), 345–358. 10.1038/nrc.2016.37
3. Garbe C, et al. (2016). Diagnosis and treatment of melanoma. European consensus-based Interdisciplinary Guideline – Update 2016. European Journal of Cancer, 63, 201–217. 10.1016/j.ejca.2016.05.005 [PubMed: 27367293]
4. Akbani R, et al. (2015). Genomic classification of cutaneous melanoma. Cell, 161(7), 1681–1696. 10.1016/j.cell.2015.05.044 [PubMed: 26091043]
5. Luke JJ, et al. (2017) Targeted agents and immunotherapies: optimizing outcomes in melanoma, Nat. Rev. Clin. Oncol 14 463–482, 10.1038/nrclinonc.2017.43. [PubMed: 28374786]
6. Winder M, & Virós A (2017). Mechanisms of drug resistance in melanoma. Mechanisms of Drug Resistance in Cancer Therapy, 91–108. 10.1007/164_2017_17
7. Kozar I, et al. (2019). Many ways to resistance: How melanoma cells evade targeted therapies. Biochimica et biophysica acta. Reviews on cancer, 1871(2), 313–322. 10.1016/j.bbcan.2019.02.002 [PubMed: 30776401]
8. Johannessen CM, et al. (2013). A melanocyte lineage program confers resistance to MAP kinase pathway inhibition. Nature, 504(7478), 138–142. 10.1038/nature12688 [PubMed: 24185007]
9. Gough NR (2013). Resistance through cAMP signaling. Science Signaling, 6(305). 10.1126/scisignal.2004979

10. Fattore L, et al. (2019). Single cell analysis to dissect molecular heterogeneity and disease evolution in metastatic melanoma. Cell death & disease, 10(11), 827. 10.1038/s41419-019-2048-5 [PubMed: 31672982]
11. Yang C, et al. (2021). Melanoma subpopulations that rapidly escape MAPK pathway inhibition incur DNA damage and rely on stress signalling. Nat Commun 12, 1747. 10.1038/s41467-021-21549-x [PubMed: 33741929]
12. Ho YJ, et al. (2018). Single-cell RNA-seq analysis identifies markers of resistance to targeted BRAF inhibitors in melanoma cell populations. Genome research, 28(9), 1353–1363. 10.1101/gr.234062.117 [PubMed: 30061114]
13. Su Y, et al. (2020) Multi-omic single-cell snapshots reveal multiple independent trajectories to drug tolerance in a melanoma cell line. Nat Commun 11, 2345 10.1038/s41467-020-15956-9 [PubMed: 32393797]
14. Buscà R, et al. (2000). Ras mediates the cAMP-dependent activation of extracellular signal-regulated kinases (ERKs) in melanocytes. The EMBO journal, 19(12), 2900–2910. 10.1093/emboj/19.12.2900 [PubMed: 10856235]
15. Stehle JH, et al. (1993). Adrenergic Signals Direct Rhythmic Expression of Transcriptional Repressor CREM In the Pineal Gland. Nature 365, 314–320. 10.1038/365314a0 [PubMed: 8397338]
16. Molina CA, et al. (1993). Inducibility and negative autoregulation of CREM: an alternative promoter directs the expression of ICER, an early response repressor. Cell, 75(5), 875–886. 10.1016/0092-8674(93)90532-U [PubMed: 8252624]
17. Razavi R, et al. (1998). ICER-IIγ is a tumor suppressor that mediates the antiproliferative activity of cAMP. Oncogene, 17(23), 3015–3019. 10.1038/sj.onc.1202225 [PubMed: 9881703]
18. Healey M, et al. (2013). Ras-induced melanoma transformation is associated with the proteasomal degradation of the transcriptional repressor ICER. Molecular carcinogenesis, 52(9), 692–704. 10.1002/mc.21908 [PubMed: 22488648]
19. Yehia G, et al. (2001). The Expression of Inducible cAMP Early Repressor (ICER) is Altered in Prostate Cancer Cells and Reverses the Transformed Phenotype of the LNCaP Prostate Tumor cell line. Cancer Research, 61: 6055–6059 [PubMed: 11507053]
20. Yehia G, et al. (2001). Mitogen-activated protein kinase phosphorylates and targets inducible cAMP early repressor to ubiquitin-mediated destruction. Journal of Biological Chemistry, 276(38), 35272–35279. 10.1074/jbc.M105404200
21. Mémin E, et al. (2011). Evidence that phosphorylation by the mitotic kinase Cdk1 promotes ICER monoubiquitination and nuclear delocalization. Experimental Cell Research, 317: 2490–2502. 10.1016/j.yexcr.2011.07.001 [PubMed: 21767532]
22. Nguyen KT, et al. (2018). Control of protein degradation by N-terminal acetylation and the N-end rule pathway. Experimental & molecular medicine, 50(7), 1–8. 10.1038/s12276-018-0097-y
23. Aksnes H, Drazic A, Marie M, & Arnesen T (2016). First things first: vital protein marks by N-terminal acetyltransferases. Trends in biochemical sciences, 41(9), 746–760. 10.1016/j.tibs.2016.07.005 [PubMed: 27498224]
24. Koren I, et al. (2018). The eukaryotic proteome is shaped by E3 ubiquitin ligases targeting C-terminal degrons. Cell, 173(7), 1622–1635. 10.1016/j.cell.2018.04.02833 [PubMed: 29779948]
25. Tasaki T, et al. (2012). The N-end rule pathway. Annual review of biochemistry, 81, 261–289. 10.1146/annurev-biochem-051710-093308
26. Ree R, Varland S, & Arnesen T (2018). Spotlight on protein N-terminal acetylation. Experimental & molecular medicine, 50(7), 1–13. 10.1038/s12276-018-0116-z
27. Hollebeke J, et al. (2012). N-terminal acetylation and other functions of Nα-acetyltransferases. Biological chemistry, 393(4), 291–298. 10.1515/hsz-2011-02288. [PubMed: 22718636]
28. Liszczak G, et al. (2013). Molecular basis for N-terminal acetylation by the heterodimeric NatA complex. Nature structural & molecular biology, 20(9), 1098–1105. 10.1038/nsmb.2636
29. Mullen JR, et al. (1989). Identification and characterization of genes and mutants for an N-terminal acetyltransferase from yeast. The EMBO journal, 8(7), 2067–2075. 10.1002/j.1460-2075.1989.tb03615.x [PubMed: 2551674]

30. Arnesen T, et al. (2009). Proteomics analyses reveal the evolutionary conservation and divergence of N-terminal acetyltransferases from yeast and humans. Proceedings of the National Academy of Sciences, 106(20), 8157–8162. 10.1073/pnas.0901931106

31. Arnesen T, et al. (2010). The chaperone-like protein HYPK acts together with NatA in cotranslational N-terminal acetylation and prevention of Huntingtin aggregation. Molecular and cellular biology, 30(8), 1898–1909. 10.1128/MCB.01199-09 [PubMed: 20154145]

32. Craig R, & Beavis RC (2004). TANDEM: matching proteins with tandem mass spectra. Bioinformatics (Oxford, England), 20(9), 1466–1467. 10.1093/bioinformatics/bth092

33. Gupta N, et al. (2011). Target-decoy approach and false discovery rate: when things may go wrong. Journal of the American Society for Mass Spectrometry, 22(7), 1111–1120. 10.1007/s13361-011-0139-3 [PubMed: 21953092]

34. Muñiz LC, Yehia G, Mémin E, Ratnakar PV, & Molina CA (2006). Transcriptional regulation of cyclin D2 by the PKA pathway and inducible cAMP early repressor in granulosa cells. Biology of reproduction, 75(2), 279–288. 10.1095/biolreprod.105.049486 [PubMed: 16625003]

35. Muniz L and Molina CA (2016) The transcriptional repressor ICER binds to multiple loci throughout the genome. Biochemical and Biophysical Research Communications, 478:1462–1465 (2016). 10.1016/j.bbrc.2016.08.147 [PubMed: 27590584]

36. Wilson BE, Mochon E, & Boxer LM (1996). Induction of bcl-2 expression by phosphorylated CREB proteins during B-cell activation and rescue from apoptosis. Molecular and cellular biology, 16(10), 5546–5556. 10.1128/MCB.16.10.5546 [PubMed: 8816467]

37. Tomita H, Nazmy M, Kajimoto K, Yehia G, Molina CA, & Sadoshima J (2003). Inducible cAMP early repressor (ICER) is a negative-feedback regulator of cardiac hypertrophy and an important mediator of cardiac myocyte apoptosis in response to β-adrenergic receptor stimulation. Circulation research, 93(1), 12–22. 10.1161/01.RES.0000079794.57578.F1 [PubMed: 12791704]

38. Seidl MD, et al. (2014). A novel intronic promoter of the Crem gene induces small ICER (smICER) isoforms. The FASEB Journal, 28(1), 143–152. 10.1096/fj.13-231977 [PubMed: 24022402]

39. Seidl MD, et al. (2020) Induction of ICER is superseded by smICER, challenging the impact of ICER under chronic beta-adrenergic stimulation. The FASEB Journal, 34, 11272–11291. 10.1096/fj.201902301RR [PubMed: 32602979]

40. Pati D, Meistrich ML, & Plon SE (1999). Human Cdc34 and Rad6B ubiquitin-conjugating enzymes target repressors of cyclic AMP-induced transcription for proteolysis. Molecular and cellular biology, 19(7), 5001–5013. 10.1128/MCB.19.7.5001 [PubMed: 10373550]

41. Woo C-H, Le N-T, Shishido T, Chang E, Lee H, Heo K-S, Mickelsen DM, Lu Y, McClain C, Spangenberg T, Yan, Molina CA, Yang J, Patterson C and Abe J Novel role of C terminus of Hsc70-interacting protein (CHIP) ubiquitin ligase on inhibiting cardiac apoptosis and dysfunction via regulating ERK5-mediated degradation of inducible cAMP early repressor. FASEB J, 24: 4917–4928 (2010). 10.1096/fj.10.162636 [PubMed: 20724525]

42. Lamas M, Molina C, Foulkes NS, Jansen E, & Sassone-Corsi P (1997). Ectopic ICER expression in pituitary corticotroph AtT20 cells: effects on morphology, cell cycle, and hormonal production. Molecular endocrinology (Baltimore, Md.), 11(10), 1425–1434. 10.1210/mend.11.10.9987

43. Rieder CL, & Maiato H (2004). Stuck in division or passing through: what happens when cells cannot satisfy the spindle assembly checkpoint. Developmental cell, 7(5), 637–651. 10.1016/j.devcel.2004.09.002 [PubMed: 15525526]

44. Topham CH, & Taylor SS (2013). Mitosis and apoptosis: how is the balance set?. Current opinion in cell biology, 25(6), 780–785. 10.1016/j.ceb.2013.07.003 [PubMed: 23890995]

45. Brower CS, Piatkov KI, & Varshavsky A (2013). Neurodegeneration-associated protein fragments as short-lived substrates of the N-end rule pathway. Molecular cell, 50(2), 161–171. 10.1016/j.molcel.2013.02.009 [PubMed: 23499006]

46. Shearer RF, et al. (2015). Functional Roles of the E3 Ubiquitin Ligase UBR5 in Cancer. Molecular cancer research : MCR, 13(12), 1523–1532. 10.1158/1541-7786.MCR-15-0383 [PubMed: 26464214]

47. Mao J, et al. (2017). UBR2 Enriched in p53 Deficient Mouse Bone Marrow Mesenchymal Stem Cell-Exosome Promoted Gastric Cancer Progression via Wnt/β-Catenin Pathway. Stem cells (Dayton, Ohio), 35(11), 2267–2279. 10.1002/stem.2702

48. Leboeuf D, et al. (2020). Downregulation of the Arg/N-degron Pathway Sensitizes Cancer Cells to Chemotherapy In Vivo. Molecular therapy : the journal of the American Society of Gene Therapy, 28(4), 1092–1104. 10.1016/j.ymthe.2020.01.021 [PubMed: 32087767]

49. Kalvik TV, & Arnesen T (2013). Protein N-terminal acetyltransferases in cancer. Oncogene, 32(3), 269–276. 10.1038/onc.2012.82 [PubMed: 22391571]

50. Linē A, et al. (2002). Serological identification and expression analysis of gastric cancer-associated genes. British journal of cancer, 86(11), 1824–1830. 10.1038/sj.bjc.6600321 [PubMed: 12087473]

Highlights

- The N-terminus of ICER is important for ICER's regulation
- NARG1 and UBR4 interact with ICER
- Altering ICER's N-terminus increases its half-life and elicits apoptosis

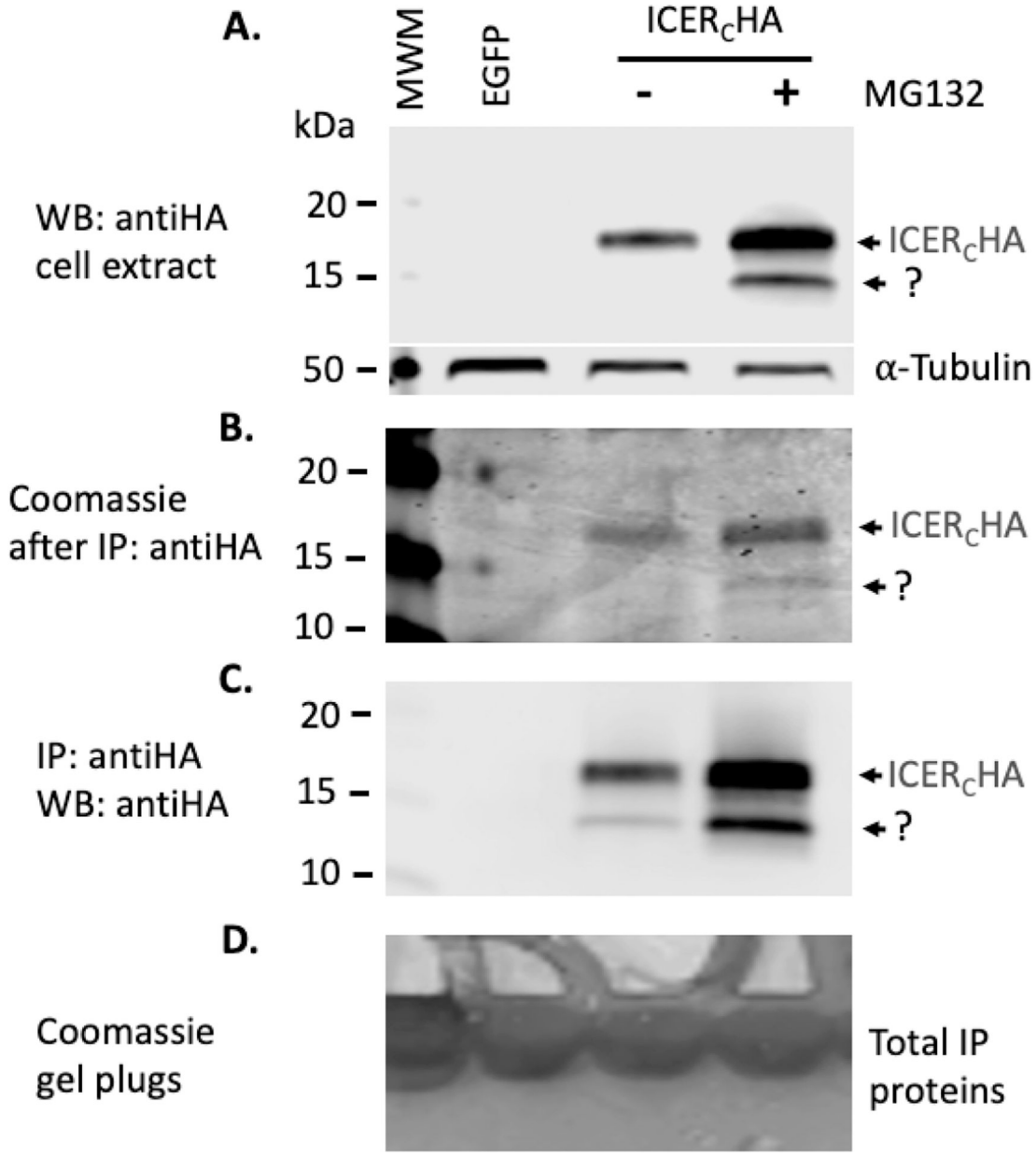

Figure 1.

Sample preparation for MS analysis. **A**. WB verification of $ICER_CHA$ expression from total cell extracts of transfected Sk-Mel-24 cells. Cells were transfected as indicated with plasmids for the expression of EGFP or $ICER_CHA$. Cells were treated (+) or not (−) with MG132 as indicated. **B**. Quantified levels of $ICER_CHA$ expression after IP with antiHA agarose-linked beads and Coomassie blue staining of the SDS-PAGE. **C**. Verification of purified $ICER_CHA$ expression from an aliquot from sample prepared as described in B. **D**. Samples were immunoprecipitated as in B and subjected to a short SDS-PAGE (10 minutes).Total IP proteins were stained with Coomassie blue. MWM indicated standard molecular weight markers in kilodaltons (KDa). The expression of α-tubulin was determined by WB as loading control.

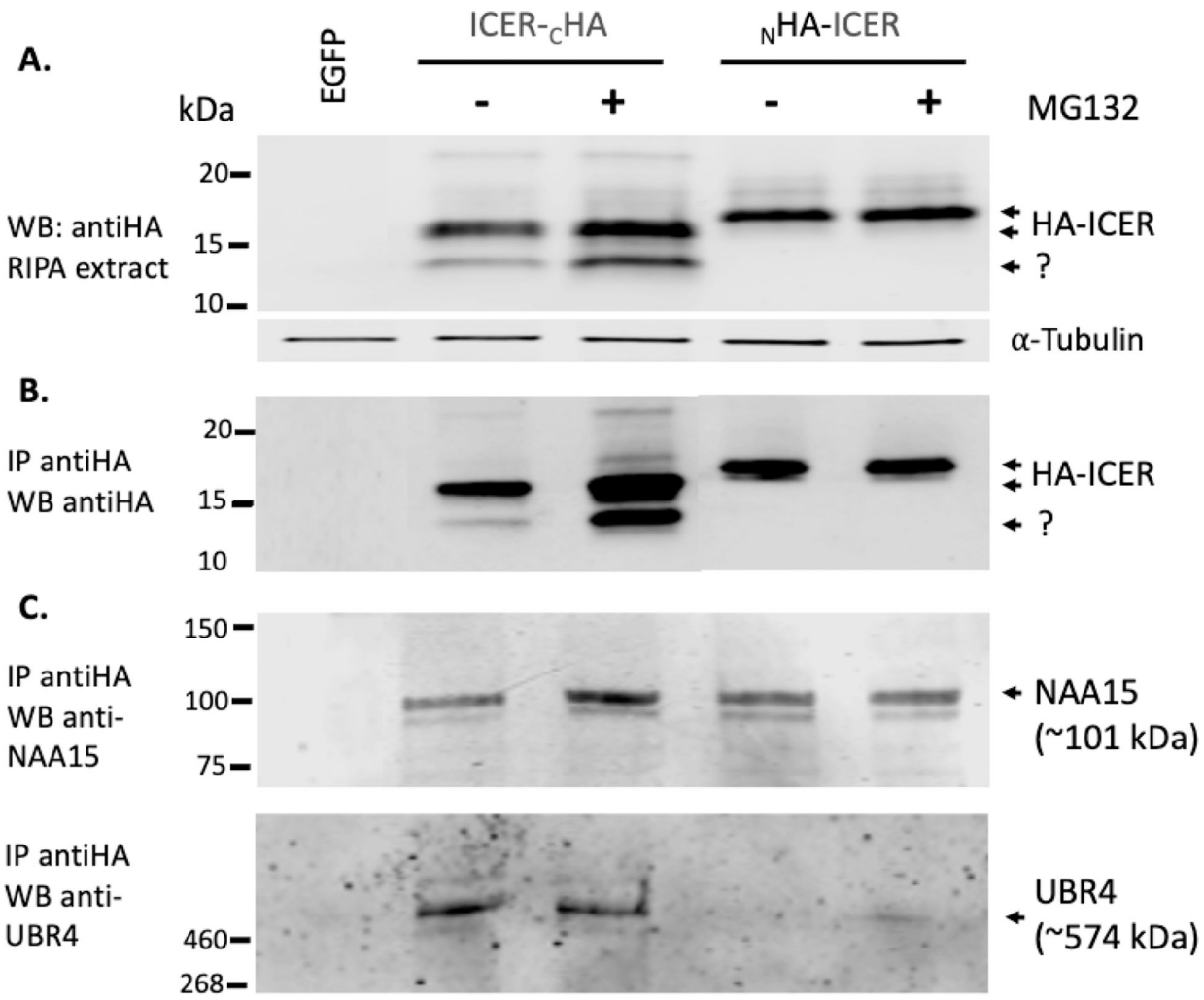

Figure 2.

Verification of ICER-interacting proteins by Co-IP and WB analysis. **A**. WB verification of ICER expression from total cell extracts of transfected Sk-Mel-24 cells. Cells were transfected as indicated with plasmids for the expression of EGFP, $ICER_CHA$ or $_NHA$-ICER. Cells were treated (+) or not (–) with MG132 as indicated. **B**. Quantified levels of ICER expression after IP with antiHA agarose-linked beads and Coomassie blue staining of the SDS-PAGE. **C**. WB analysis of NAA15 and UBR4 after IP with antiHA agarose-linked beads from transfected cells. The relative mobility of standard molecular weight markers in kilodaltons (KDa) is indicated. The expression of α-tubulin was determined by WB as loading control.

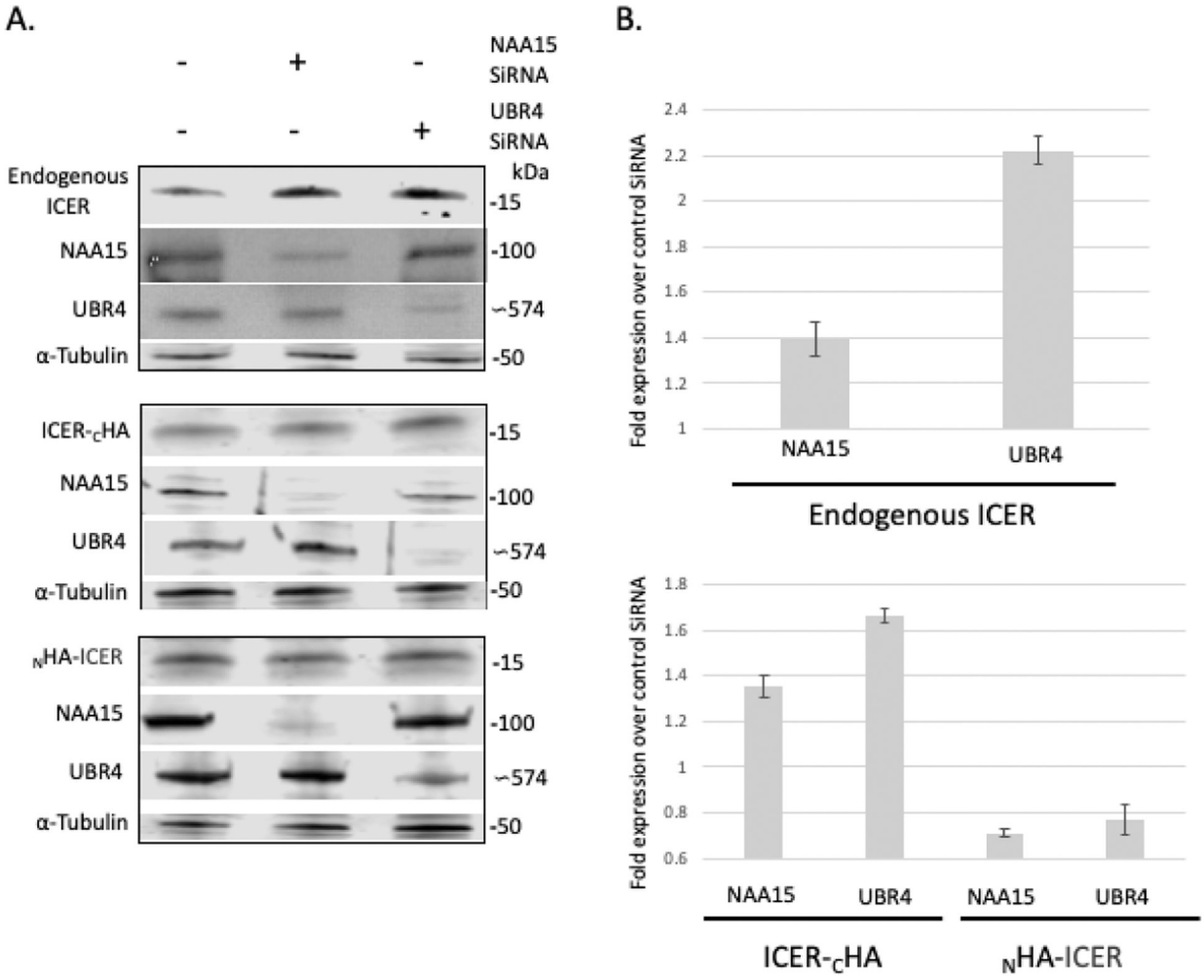

Figure 3.

ICER levels after gene silencing of NAA15 and UBR4 by siRNA. **A**. Representative WBs to determine the levels of endogenous and transfected ICER and to verify successful reduction in expression of NAA15 and UBR4 after siRNA gene silencing. Cells were transfected with the indicated siRNAs (+), or as a control (−) with Silencer™ Negative Control No. 1 siRNA as indicated in the Materials and methods section. The expression of α-tubulin was determined by WB as loading control. The relative mobility of proteins in kilodaltons (KDa) is indicated. **B**. Fold expression of endogenous or transfected ($ICER_CHA$ and $_NHA$-ICER) levels of ICER after NAA15 and UBR4 gene silencing. The densitometric values for the bands of samples transfected with experimental siRNA were expressed as a function of the samples transfected with control siRNA. Values shown are means −/+ S.E. (n=3 independent experiments).

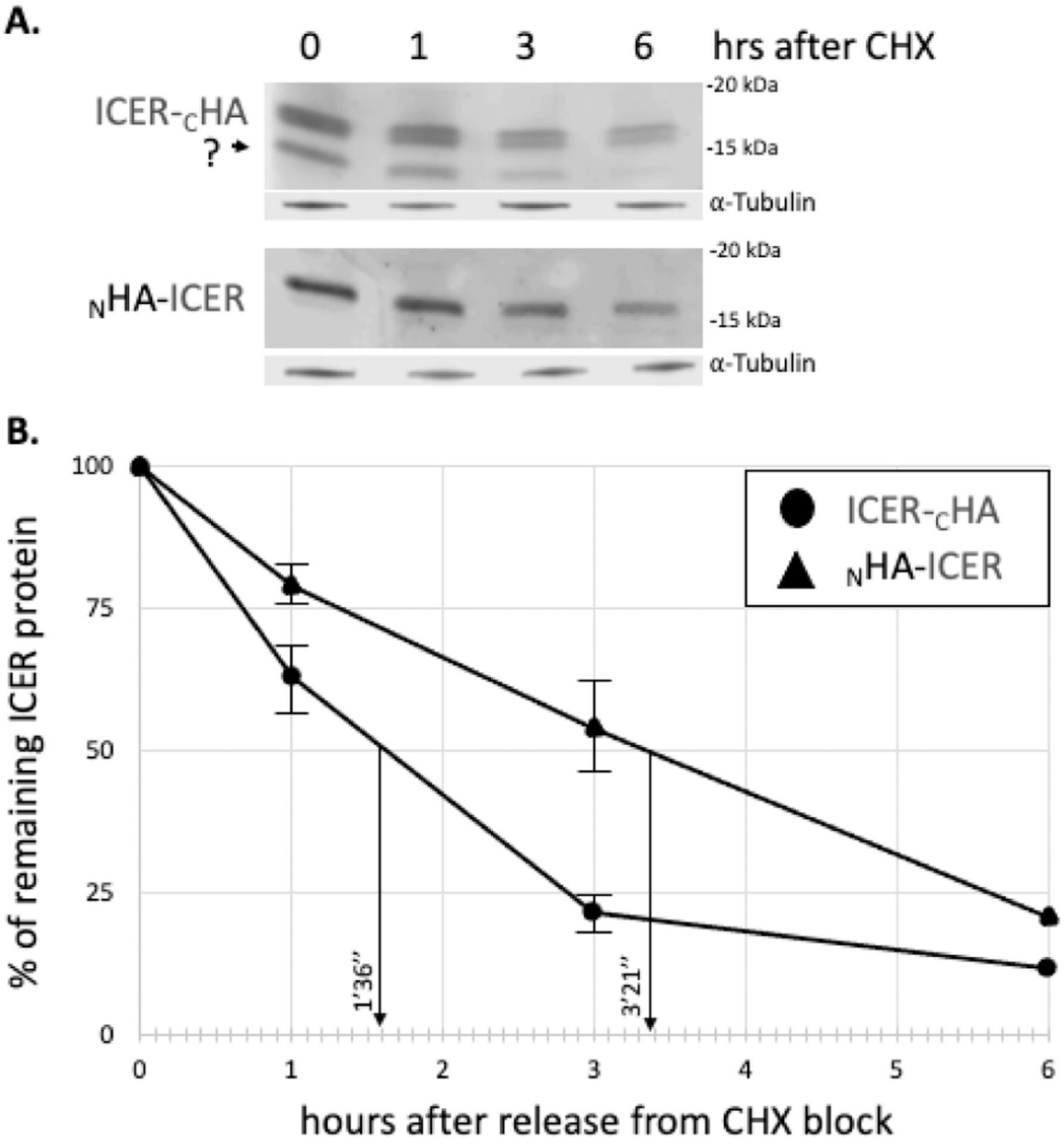

Figure 4.

$ICER_CHA$ and $_NHA$-ICER protein half-life. Half-life experiments were performed as described under Materials and methods. Cells were transiently transfected with pcDNA3.1(+)-$ICER_CHA$ or -$_NHA$-ICER. Transfected cells were treated with cycloheximide, samples collected at indicated times after treatment and Western blot performed. HA-ICER and α-tubulin protein levels were quantified and values expressed as a function of α-tubulin for each time point. The relative mobility of proteins in kilodaltons (KDa) is indicated. Values shown are means −/+ S.E. (n=3 independent experiments).

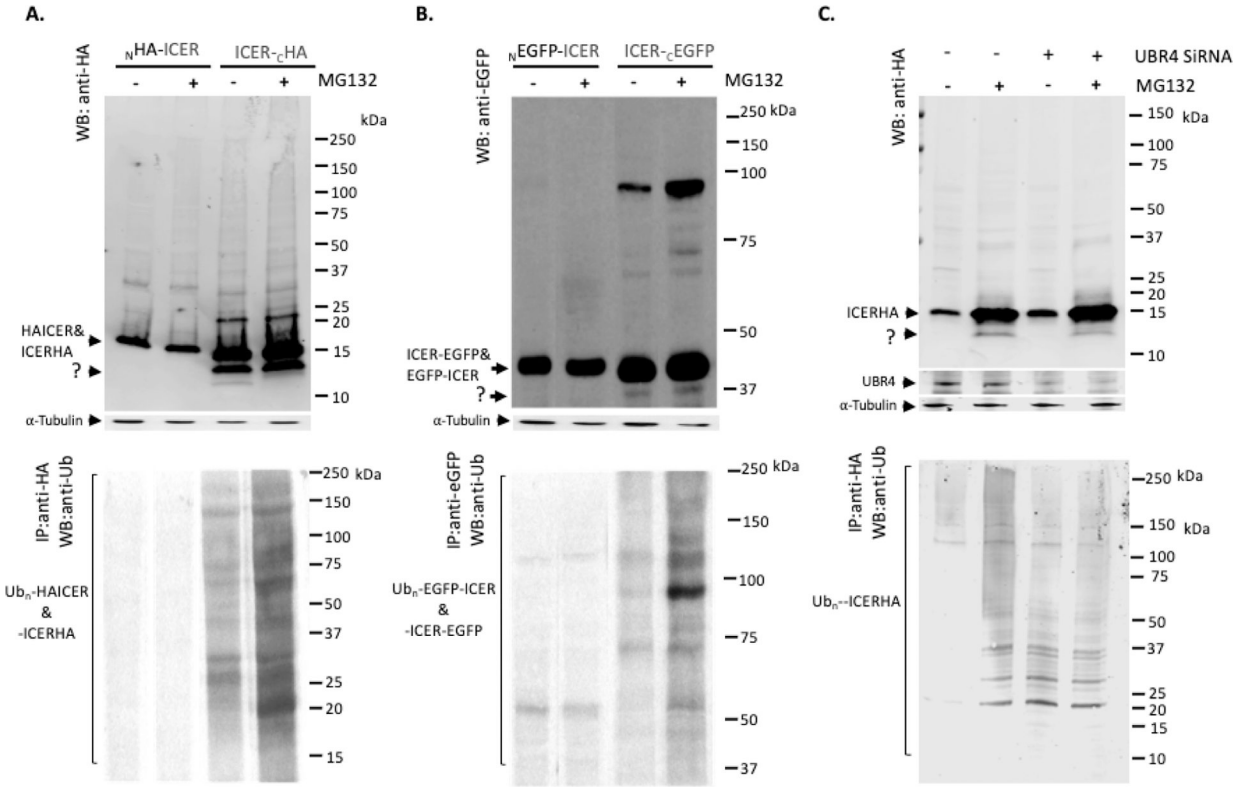

Figure 5.

Ubiquitin-mediated proteasomal regulation of $ICER_CHA$ and $_NHA$-ICER by UBR4. **A., B.** and **C.** cells were transfected as indicated with plasmids for the expression of $_NHA$-ICER, $ICER_CHA$, $_NEGFP$-ICER and $ICER_CEGFP$, and cells were treated (+) or not (−) with MG132 as indicated. **C.** Cells were transfected with the UBR4 siRNAs (+), or as a control (−) with Silencer™ Negative Control No. 1 siRNA as indicated in the Materials and methods section. Top panels: the expression of the transfected constructs was determined by WB with anti-HA or anti-EGFP as described in the Methods section. Bottom panel: the expression of ubiquitinated transfected constructs was determined by WB with antiUb antibodies after immunoprecipitated with anti-HA or anti-EGFP antibodies as described in the Methods section. The relative mobility of standard molecular weight markers in kilodaltons (KDa) is indicated. The expression of α-tubulin was determined by WB as loading control.

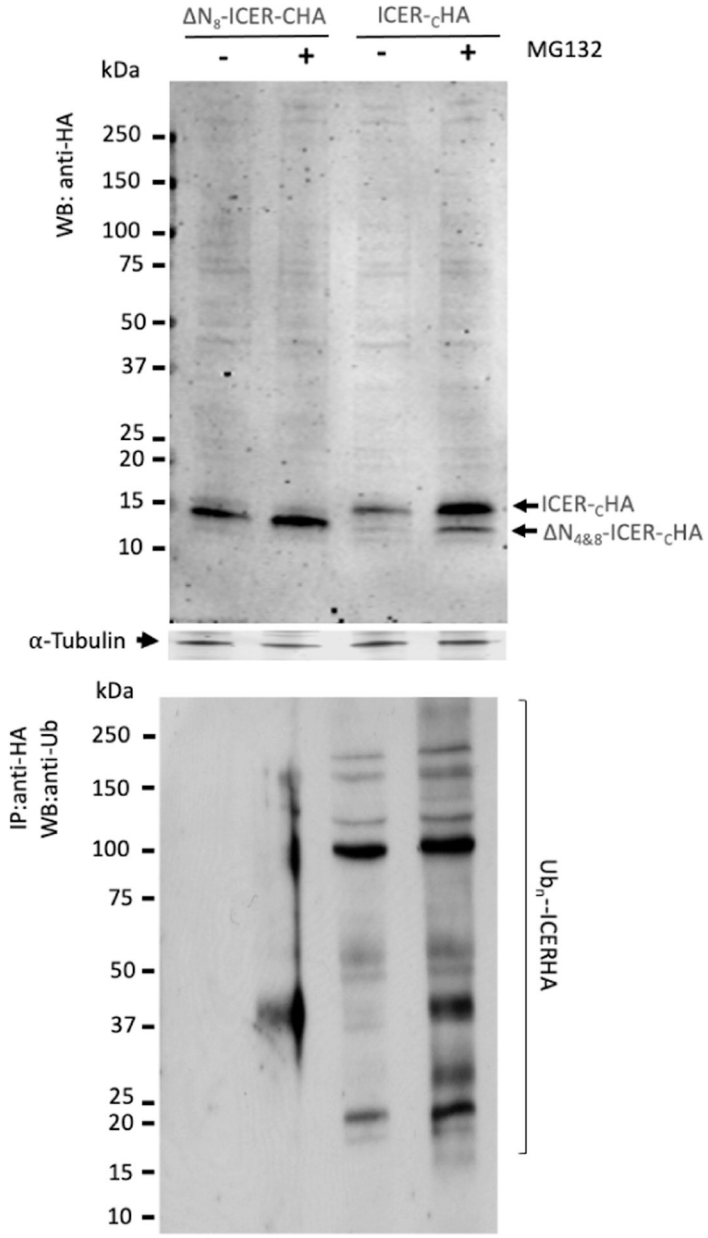

Figure 6.

Role of the N-terminus of ICER on ubiquitin-mediated proteasomal degradation. **A**. cells were transiently transfected with pcDNA3.1(+)-ICER$_C$HA or −Δ$_8$N-ICER$_C$HA and cells were treated (+) or not (−) with MG132 as indicated. Upper panel: the expression of the transfected constructs was determined by WB with anti-HA as described in the Methods section. Lower panel: the expression of ubiquitinated transfected constructs was determined by WB with antiUb antibodies after immunoprecipitated with anti-HA or anti-EGFP antibodies as described in the Methods section. The relative mobility of standard molecular weight markers in kilodaltons (KDa) is indicated.

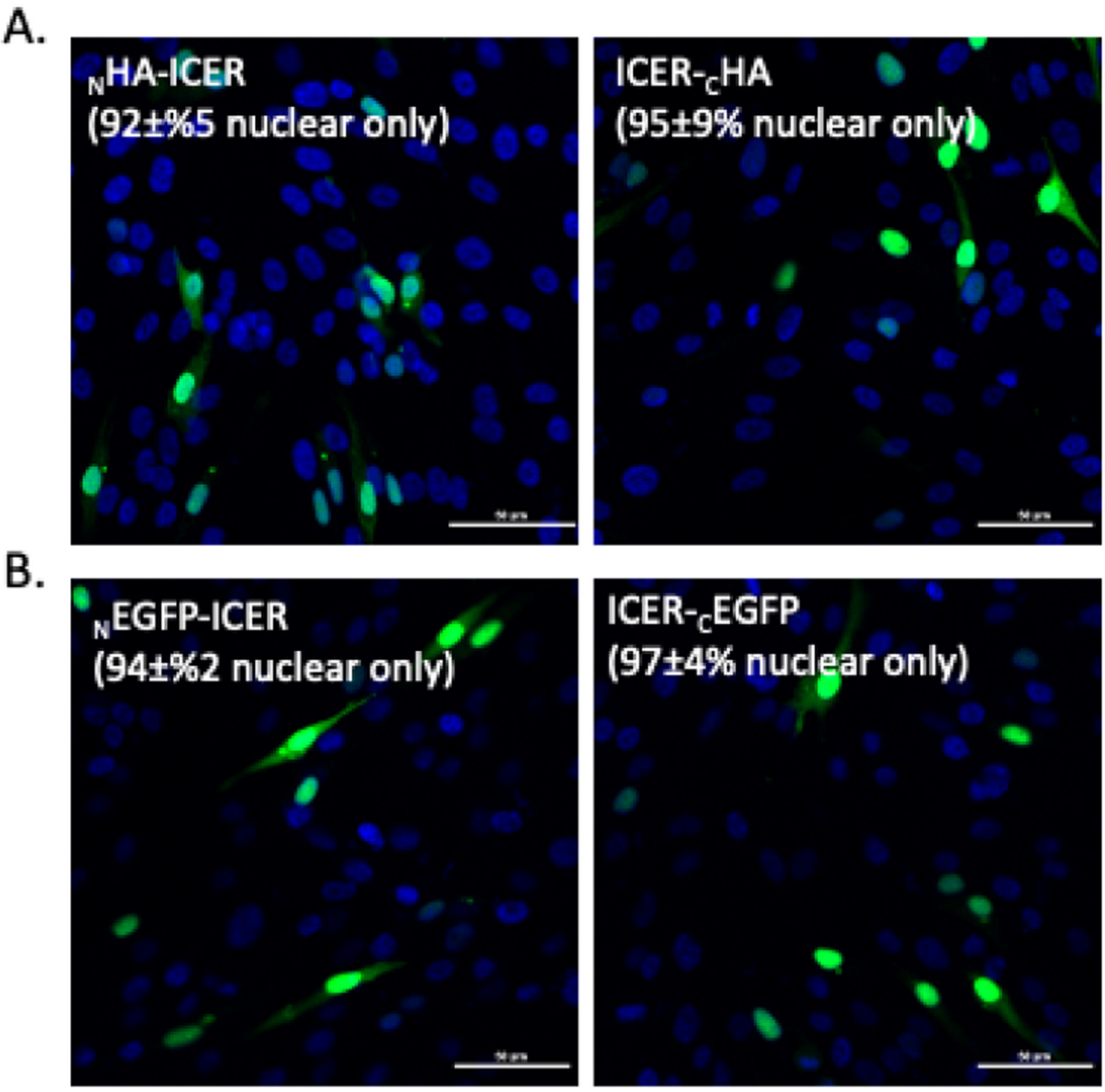

Figure 7.

$_N$HA-ICER, ICER$_C$HA, $_N$EGFP-ICER and ICER$_C$EGFP subcellular localization. **A.** and **B.**, cells were transiently transfected with pcDNA3.1(+)-$_N$HA-ICER, -ICER$_C$HA, -$_N$EGFP-ICER or -ICER$_C$EGFP as indicated. **A.** ICC was performed as described under Materials and methods. ICER-positive cells were visualized by fluorescence microscopy. **B.** EGFP-positive cells were visualized by direct fluorescence microscopy. Percent nuclear (nuclear only) was calculated by counting the number of cells with nuclear signal divided by the total number of ICC- or EGFP- positive cells. Values shown are means −/+ S.E. (n=3 independent counting areas of more than 30 positive cells).

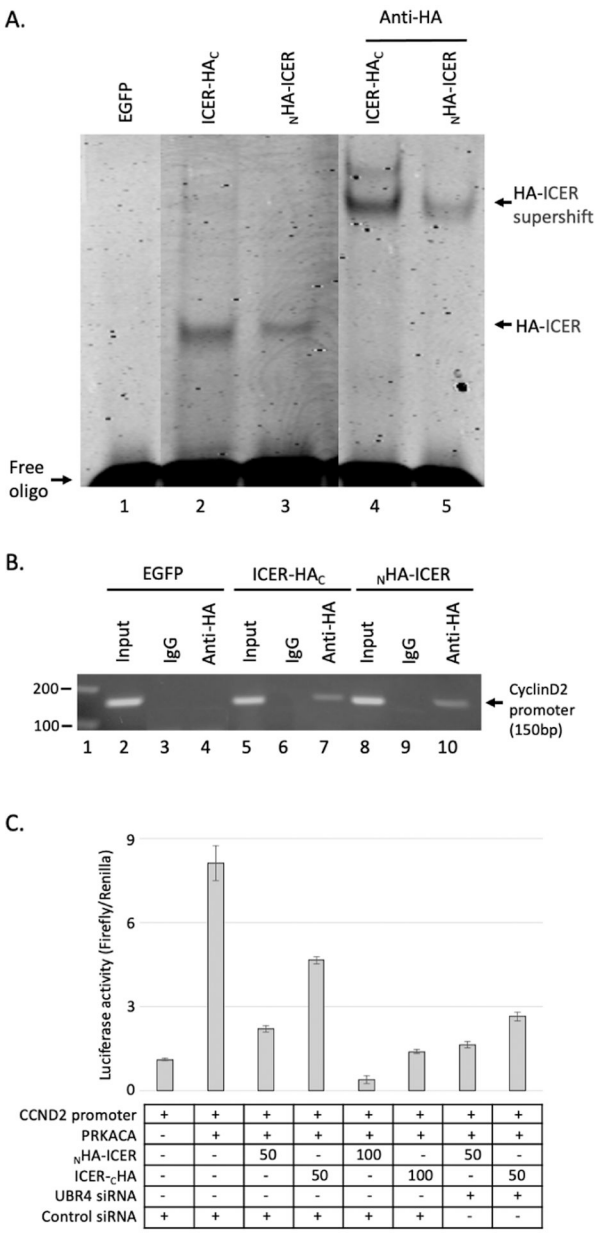

Figure 8.

DNA binding and transcriptional repressor function of ICER$_C$HA and $_N$HA-ICER. **A.** Cells were transiently transfected with pEGFP, pcDNA3.1(+)-ICER$_C$HA or -$_N$HA-ICER, HAICER was IP and EMSA was performed as described under Materials and methods. **B**. Cells were transiently transfected with pEGFP, pcDNA3.1(+)-ICER$_C$HA or -$_N$HA-ICER, HA-ICER and ChIP was performed as described under Materials and methods. “Input” represents PCR before IP. **C**. Luciferase activity was measured in transiently transfected cells (+) with a plasmids expressing the luciferase reporter gene containing 962 base pairs fragment of the human cyclin D1 promoter (CCND2) the catalytic subunit of PKA (PRKACA), 50 or 100ng of pcDNA3.1(+)-ICER$_C$HA or -$_N$HA-ICER. Cells were also transfected with the UBR4 siRNAs (+), or as a control (−) with SilencerTM Negative

Control No. 1 siRNA as indicated in the Materials and methods section. A renilla luciferase vector was used to normalize for transfection efficiency; relative luciferase activity is expressed as a ratio of firefly:renilla. Data are presented as the mean of 3 independent experiments.

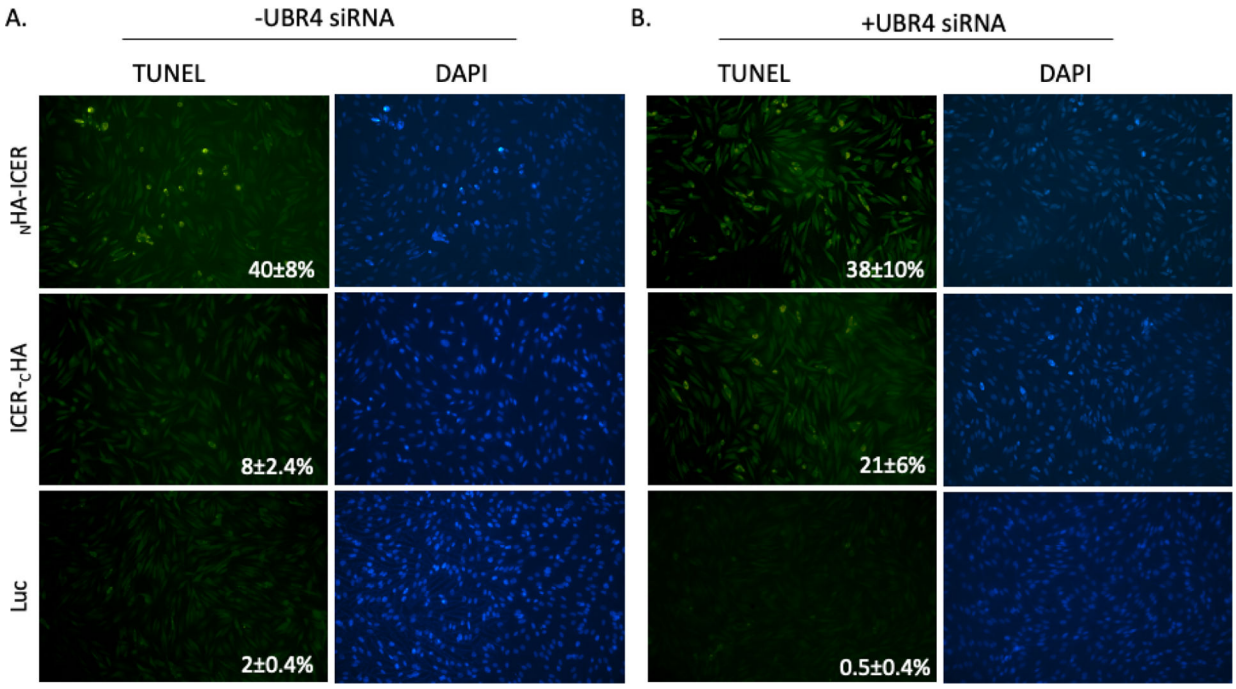

Figure 9.

TUNEL assay to measure fragmented DNA of apoptotic cells. **A. and B.**, Cells were transiently transfected with pcDNA3.1(+)-ICER$_C$HA, -$_N$HA-ICER or -Luciferase (Luc) as a control. **B**. Cells were also transfected with the UBR4 siRNAs (+ BRR4 siRNA) as indicated in the Materials and methods section. Forty eight hours after transfection cells were analyzed for TUNEL as described in the Materials and methods section. Percent of TUNEL positive cells was calculated by counting the number of TUNEL positive signals divided by the total number of total cells (DAPI) and normalized to transfection efficiency determined by EGFP expression in parallel transfection experiments. Values shown are means −/+ S.E. (n=6 independent counting areas of positive cells).

Table 1.

Spectral counts of ICER$_C$HA-interacting proteins after mass spec analysis of co-immunoprecipitated peptides, in the absence (−PI) or presence (+PI) of proteasome inhibitor MG132. Control cells were transfected with pEGFPN1 and processed and analyzed as experimental samples (ICER$_C$HA (−PI) and ICER$_C$HA (+PI). The data shown is a compilation of 3 independent experiments.

UniProtKB	description	EGFP	ICERcHA (−PI)	ICERcHA (+PI)
sp|P78527|PRKDC_HUMAN	DNA-dependent protein kinase catalytic subunit	4	19	67
sp|P16070|CD44_HUMAN	CD44 antigen; CDw44	6	15	29
sp|Q14204|DYHC1_HUMAN	Cytoplasmic dynein 1 heavy chain 1		10	35
sp|P0DMV9|HS71B_HUMAN	Heat shock 70 kDa protein 1B	3	3	26
sp|Q9BXJ9|NAA15_HUMAN	N-alpha-acetyltransferase 15 NAA15)		6	25
sp|P21589|5NTD_HUMAN	5—-nucleotidase; 5—-NT	3	9	15
sp|Q9UJV9|DDX41_HUMAN	Probable ATP-dependent RNA helicase DDX41	1		11
sp|P31151|S10A7_HUMAN	Protein S100-A7; Psoriasin	1	3	13
sp|P51784|UBP11_HUMAN	Ubiquitin carboxyl-terminal hydrolase 11		13	8
sp|P05090|APOD_HUMAN	Apolipoprotein D; Apo-D	1	4	12
sp|P38646|GRP75_HUMAN	Stress-70 protein	1	4	10
sp|P29508|SPB3_HUMAN	Serpin B3	2		14
sp|P41252|SYIC_HUMAN	Isoleucine--tRNA ligase	1	3	11
sp|Q86VP6|CAND1_HUMAN	Cullin-associated NEDD8-dissociated protein 1			15
sp|Q92616|GCN1_HUMAN	eIF-2-alpha kinase activator GCN1		2	11
sp|Q92973|TNPO1_HUMAN	Transportin-1; Importin beta-2; Karyopherin beta-2		5	7
tr|G5E998|G5E998_HUMAN	cAMP-responsive element modulator	1	1	7
sp|P20618|PSB1_HUMAN	Proteasome subunit beta type-1		2	6
sp|P25788|PSA3_HUMAN	Proteasome subunit alpha type-3	2	2	5
sp|P28074|PSB5_HUMAN	Proteasome subunit beta type-5	2		5
sp|P26640|SYVC_HUMAN	Valine--tRNA ligase		1	7
sp|O60832|DKC1_HUMAN	H/ACA ribonucleoprotein complex subunit DKC1		2	4
sp|P43490|NAMPT_HUMAN	Nicotinamide phosphoribosyltransferase		1	6
sp|Q14974|IMB1_HUMAN	Importin subunit beta-1; lmportin-90			6
sp|Q15843|NEDD8_HUMAN	NEDD8; Neddylin			4
sp|Q5T4S7|UBR4_HUMAN	E3 ubiquitin-protein ligase UBR4			3
sp|O95373|IPO7_HUMAN	Importin-7; Imp7; Ran-binding protein 7; RanBP7			4
sp|P09668|CATH_HUMAN	Pro-cathepsin H			4